19th INTERNATIONAL CONGRESS ON ACOUSTICS
MADRID, 2-7 SEPTEMBER 2007

SOUND PROPAGATION AND BUBBLE MOTION IN A CAVITATING CHANNEL

PACS: 43.35.Ei

Mettin, Robert[1], Claussen, Jann-Ohle[1]; Campos-Pozuelo, Cleofé[2]
[1] Drittes Physikalisches Institut, Universität Göttingen, Friedrich-Hund-Platz 1, 37077 Göttingen, Germany; R.Mettin@physik3.gwdg.de
[2] Instituto de Acústica, CSIC, C/Serrano, 144, Madrid, E-28006, Spain; ccampos@ia.cetef.csic.es

ABSTRACT
The acoustic field and the emergence, distribution, and motion of bubbles in two rectangular water channels is investigated at ultrasonic frequencies around 20 kHz. The transducers are positioned at one channel end. We identify a near-field and a far-field region by measuring amplitude and phase of the acoustic pressure within the channels at low intensity. At higher ultrasonic power, cavitation bubbles close to the transducer show net drift into the channel, while bubbles in the far field form streamers fixed in space. Inbetween, a hopping bubble motion is observed. This can be reproduced by a calculation of bubble drift taking into account Bjerknes forces and rectified gas diffusion into the bubbles.

INTRODUCTION
The modeling of cavitating liquids is still a challenging task. Complicating aspects are a wide range of temporal and spatial scales, nonlinearity, and granularity. The latter expression stands for the fact that spatial averages over bubble densities in cavitating regions are not always well defined, and a description on the basis of single bubbles is beneficial. In particular in acoustic cavitation, bubbles are known to be distributed quite inhomogenously, forming streamers [1] and other structures [2]. Consequently, some modeling of bubble distributions has been based on single bubble (or "particle") approaches [3]. On the other hand, in low frequency ultrasonic cavitation, the bubble sizes are typically much smaller than the wavelengths, and the description of the sound field on basis of spatial averages is a reasonable and common attempt [4,5]. In recent work, also combinations of discrete (bubble) and continuous (sound field) description has been employed successfully for specific problems [6]. Nevertheless, there is still a lack of experimental data and validation of models in the area of acoustically cavitating liquids. This is the motivation for the proposed investigation of cavitation in acoustic waveguides (sound channels). The work aims at the observation of cavitating sites and bubble motion, and at the influence of strong cavitation on the sound propagation in the channel. Experiments are ongoing, but first results are presented in this paper.

CHANNEL SET-UP
Observations and measurements have been carried out in two transparent water channels of similar type. The larger one ("Madrid" channel, no figure shown) has an inner length of 71 cm, inner width of 5 cm, and an inner wall height of 7 cm. The walls and the bottom are made of 2 cm thick PMMA, and at one end a piezoelectric sandwich transducer, operating at 19.5 kHz is attached. The second ("Göttingen") channel has the inner dimensions of 4.6 x 4.6 x 20 cm^3, with 0.2 cm PMMA walls (Fig.1). At both ends piezoelectric sandwich transducers (ELMA GmbH, Singen, Germany) are attached, working at 25 kHz. Only one transducer is used in these experiments.
The channel widths and heights are in the range of the (free field) acoustic wavelengths, and therefore the wave propagation is bound to distinct (*m,n*) modes [7]. The limiting water level *H* for the (*m,n*) mode can be calculated from

$$H^{(m,n)} = m/\sqrt{4f^2/c_0^2 - n^2/w^2},$$

where *f*, c_0, and *w* stand for the acoustic frequency, the (free) sound speed, and the channel width. This yields that for the Madrid (Göttingen) channel, the (1,1) mode is propagating above $H^{(1,1)}$ = 4.2 cm (3.7 cm), and it is the only propagating mode below $H^{(1,2)}$ = 7.1 cm ($H^{(2,1)}$ = 7.4

cm). For this calculation, the PMMA walls were considered equivalent to water, thus adding to the (real) water width and height. In summary, both channels are constructed to have the sound propagation bound to the (1,1) mode, or no propagation at all (below $H^{(1,1)}$).

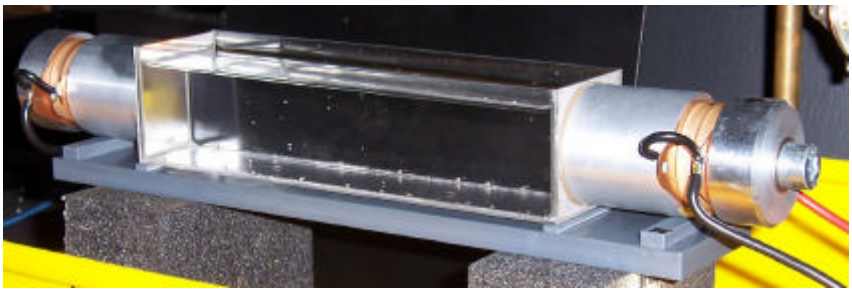

Figure 1.- Rectangular PMMA “Göttingen” channel with sandwich transducers.

SOUND FIELD MEASUREMENTS

The field is generally split into a near field in front of the transducer and a standing wave region in the rear part of the channel. The near field has a traveling wave character, and the pressure phase is varying continuously. The distant field has a pronounced standing wave character, as the amplitude shows localized maxima and minima, and the pressure phase is jumping 180 deg at the minima. This can also be seen in an FEM simulation of the Göttingen channel, given in

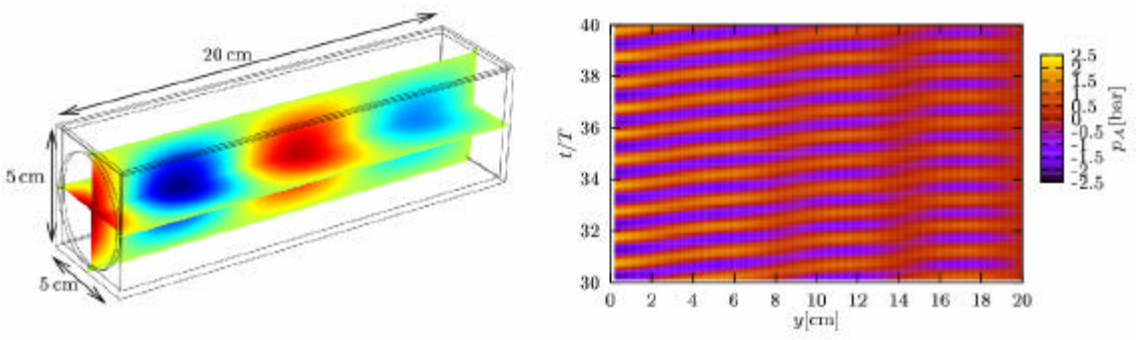

Fig. 2.

Figure 2.- Finite Element calculation of the sound wave inside the Göttingen channel. Left: Momentary pressure in the 3D geometry; transducer at the left end (not plotted). Right: Pressure on the center axis vs. time, showing a decaying amplitude from left to right and a continuously varying phase at the left (transducer) side. At the right channel end, the phase becomes flat.

For driving voltages below the cavitation threshold, the pressure amplitude and phase has been measured experimentally by two hydrophones to determine the standing and traveling wave shares in the Madrid channel. We define the length d of the near field as the distance from the transducer beyond which a clear phase jumping can be observed. This length shows a strong dependence on the water filling height h, see Fig. 3. To understand this, let us first consider the acoustic near field of a piston source in a half space that is approximated by $r_{NF}=S/\lambda$, S being the transducer area and λ the wavelength [8]. In our set-up, the guiding channel walls lead to propagation in the (1,1) mode, and therefore we have to use its wavelength, given by $\lambda^{(1,1)}=c_{ph}/f$. The phase velocity c_{ph} of the (1,1) mode is calculated by

$$c_{ph}^{(1,1)}=c_0/\sqrt{1-(c_0/2f)^2(w^{-2}+h^{-2})}$$

and diverges if the water level h is reduced down to the limiting height $H(1,1)$. Accordingly, the (1,1) mode wavelength diverges, and the near field (or traveling wave) region shrinks to zero for the water level falling to $H^{(1,1)}$. Additionally, we have to take into account “mirror” sources because of the reflecting walls. This increases the transducer area S to a “virtual” area $S_v = bS$ by some factor $\beta>1$. Without investigating this issue further here, we expect the near field to be extended in the same way by β due to this. Indeed, the measurements of d in the Madrid

channel can be fitted quite well to the modified near field distance $\beta r_{NF} = \beta S/\lambda^{(1,1)}$ with β=20, shown in Fig. 3. Note that the (real) water level *H* given in the figure has to be added to the 2 cm of PMMA. This leads to an observed "virtual" cutoff water height of about 4.5 cm, close to the theoretical $H^{(1,1)}$ = 4.2 cm.

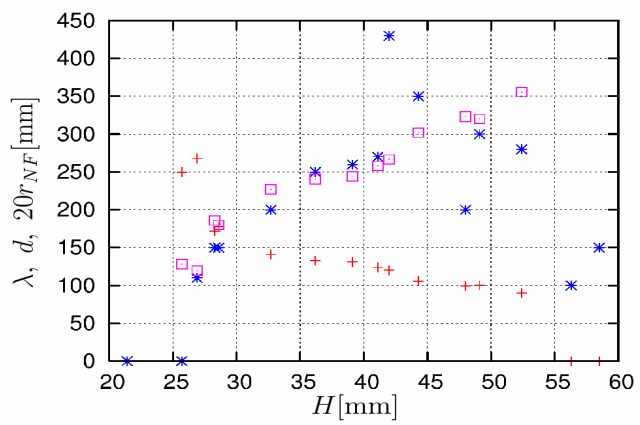

Figure 3.- Measurements in the Madrid channel: wavelength λ of the (1,1) mode (red crosses), near field (traveling wave) distance *d* (blue stars), and theoretical piston source near field length, r_{NF}, scaled with a factor of 20 (pink squares).

BUBBLE MOTION

For higher sound pressure levels, cavitation sets in, and bubbles appear at or close to the transducer. The bubble motion is first directed away from the transducer, and streamer filaments are visible more or less in parallel to the channel axis. After some centimeters, the bubbles can stop and form streamers vertical to the channel axis (in parallel to the transducer plane). To the rear end of the channel, more perpendicular streamer structures appear in regular distances, fitting to the standing wave pressure structure. From time to time, single bubbles, bubble clouds, or whole filaments that have been fixed to such a vertical plane can start a motion along the channel direction again. Then a kind of hopping motion is observed, and the single bubbles involved appear to grow in size. Figure 4 shows a scetch of this hopping bubble motion.

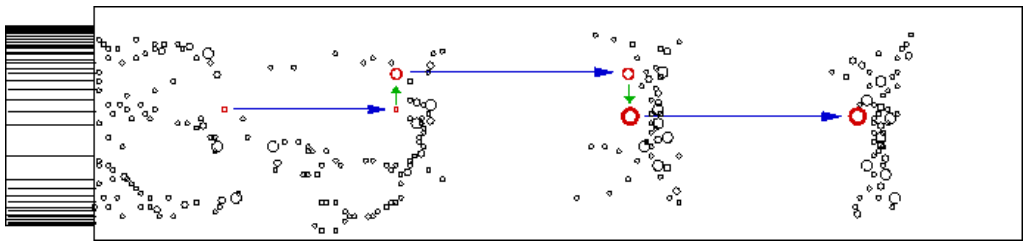

Figure 4.- Schematic drawing of the bubble structures in the channel. Close to the transducer (left) streamers in axial direction emerge. Further to the reflecting end (right), perpendicular streamers are formed. Bubbles can 'hop' between bubbly regions by a translation – diffusion process, which is shown by the red bubble: blue arrows indicate motion due to Bjerknes forces, green arrows mark diffusional growth without large net motion (bubble sizes schematically and not to scale).

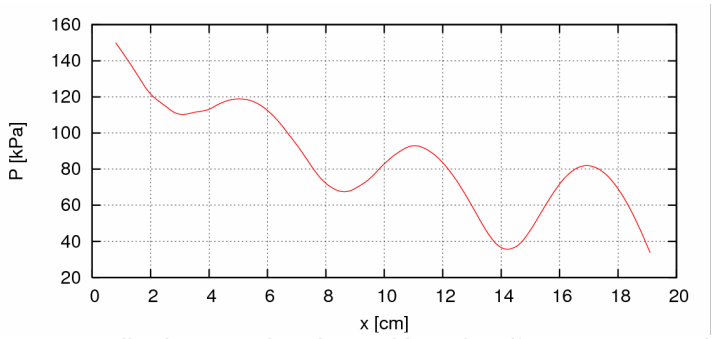

Figure 5.- Pressure amplitude *P* vs. the channel length *x* (from an FEM calculation of the Göttingen channel similar to Fig.2). The value of *P* is given for the channel axis.

We have modeled the bubble motion on the channel axis by a particle approach, including the primary Bjerknes force and rectified gas diffusion [9,10]. The underlying sound field parameters have been taken from an FEM simulation (without bubbles) of the Göttingen channel. The pressure amplitude is shown in Fig. 5: A decaying, weakly modulated part in front of the transducer (left) is developing into a standing wave with higher contrast (right). In the calculation, nonlinear spherical bubble oscillations and amplitude and phase terms of the primary Bjerknes force have been taken into account. Rectified diffusion has been calculated according to Eller and Flynn [11,10]. Bubbles of different initial equilibrium radii are put into the simulation at the transducer position, $x = 0$. A fast translation begins until a positional equilibrium is reached at about $x = 8.5$ cm. The bubbles stay at this location until they have grown by rectified diffusion to about 50 µm size. Then, they translate again forward until about $x = 11$ cm. This scenario is depicted in Fig. 6(a)-(d). It is interesting to note that the sizes adjust to the same value by this translation-diffusion mechanism, and therefore the bubble population becomes equilibrated.

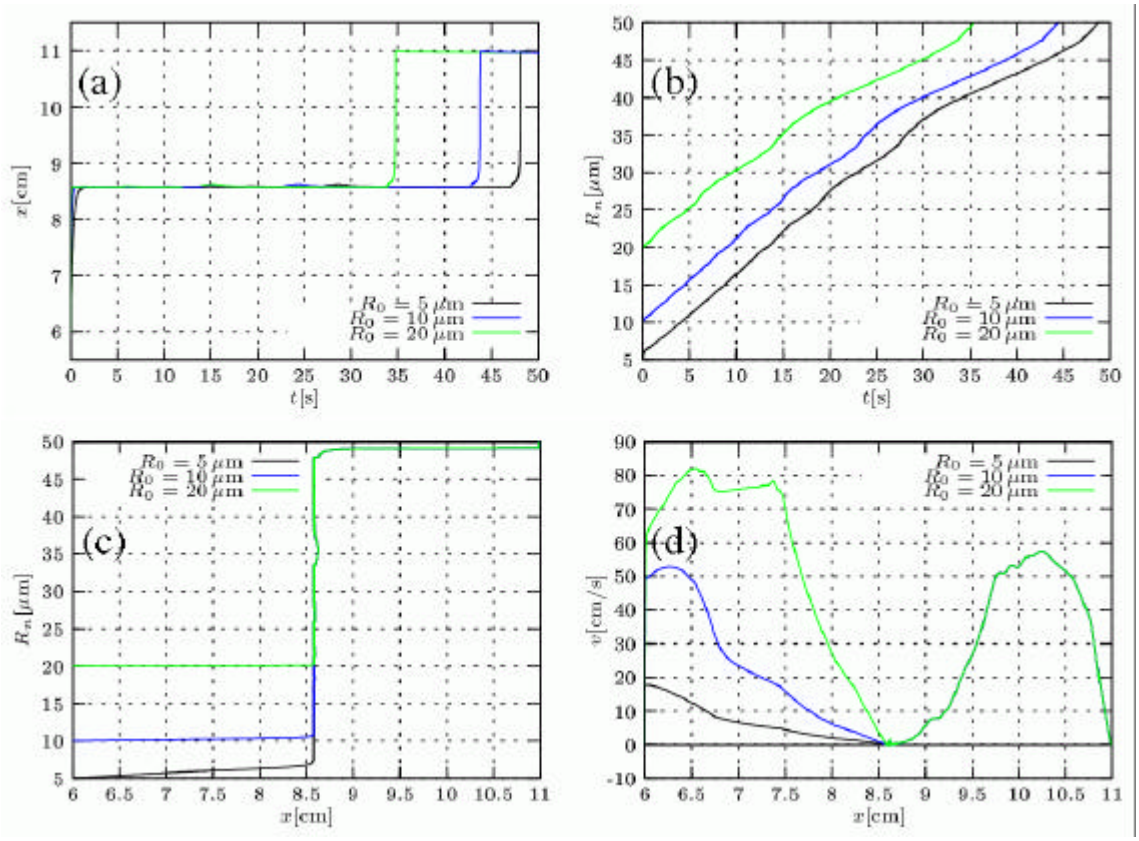

Figure 6.-Translation and rectified diffusion of bubbles in the channel sound field on the horizontal axis, according to Fig. 5. The colors indicate different initial bubble sizes. (a): Bubble

position x vs. time t. (b): Momentary bubble equilibrium radii R_n vs. time t. (c): R_n vs. position x. (d): Bubble translation velocity v vs. position x.

CONCLUSION AND OUTLOOK

We have reported on preliminary observations, measurements, and calculations of acoustic cavitation in elongated rectangular channels with sound soft walls. The sound field has been characterized to consist roughly of a near field part with decaying pressure amplitude and smoothly varying pressure phase, and a far field which is more developed into a standing wave with strongly modulated amplitude and constant phase. The length of the near field has been measured to scale inversely with the phase velocity of the propagating (1,1) mode, and theoretical reasoning has been given in terms of the piston source near field length, multiplied by some factor because of mirror sources. For the cavitating case, bubble distribution and motion has been investigated visually: bubbles are driven away from the transducer, forming streamers in axial direction, and gather later in the channel in streamer structures perpendicular to the channel axis. Bubbles can show a hopping motion away from the transducer, resting for intervals of the order up to seconds at roughly the same position. This can be explained by translation due to primary Bjerknes forces, and rectified diffusion on a slower time scale at the rest positions. After growing to a certain bubble equilibrium size R_n, the rest position becomes unstable, and translation starts again. By this mechanism, the bubble population can become equilibrated to similar values of R_n to a certain extent. Calculations by a particle model approach can produce hopping behavior of bubbles in the simulated pressure field of a channel. Prospective investigations will focus on stronger cavitation in the channels, leading possibly to a significant back reaction of the bubbles on the sound field distribution. This will be exploited to extend and validate numerical models of sound propagation in cavitating liquids.

References:

[1] T. G. Leighton: *The Acoustic Bubble*, Academic Press, London (UK), 1994

[2] R. Mettin: Bubble structures in acoustic cavitation. In: A. A. Doinikov (ed.): *Bubble and Particle Dynamics in Acoustic Fields: Modern Trends and Applications*, Research Signpost, Kerala (India) 2005, pp. 1-36

[3] R. Mettin, S. Luther, C.-D. Ohl, W. Lauterborn: Acoustic cavitation structures and simulations by a particle model. Ultrasonics Sonochemistry **6** (1999) 25-29

[4] L. Van Wijngaarden: On the equations of motion for mixtures of liquid and gas bubbles. J. Fluid Mech. **33** (1968) 465-474

[5] R. E. Caflisch, M. J. Miksis, G. C. Papanicolaou, L. Ting: Effective equations for wave propagation in bubbly liquids. J. Fluid Mech. **153** (1985) 259-273

[6] R. Mettin, P. Koch, W. Lauterborn, D. Krefting: Modeling acoustic cavitation with bubble redistribution. In: *Sixth International Symposium on Cavitation – CAV2006*, Wageningen, The Netherlands (2006), paper no. 75

[7] L. E. Kinsler, A. R. Frey, A. B. Coppens, J. V. Sanders: *Fundamentals of Acoustics*, John Wiley & Sons, New York (USA), 1982

[8] H. Kuttruff: *Physik und Technik des Ultraschalls*, Hirzel, Stuttgart (Germany), 1988.

[9] I. Akhatov, R. Mettin, C.D. Ohl, U. Parlitz, W. Lauterborn: Bjerknes force threshold for stable single bubble sonoluminescence. Phys. Rev. E **55** (1997) 3747-3750

[10] J. O. Claussen, R. Mettin, W. Lauterborn: Bjerkneskräfte und gleichgerichtete Diffusion in laufenden und stehenden Wellenfeldern. In: *Fortschritte der Akustik - DAGA 2007*, Stuttgart, Germany (2007)

[11] A. I. Eller, H. G. Flynn: Rectified diffusion during nonlinear pulsations of cavitation bubbles. J. Acoust. Soc. Am. **37** (1965) 493-503